

Early Tertiary volcanic rocks in Well 163/6-1A, Rockall Trough

A. C. Morton, J. E. Dixon, J. G. Fitton, R. M. Macintyre, D. K. Smythe & P. N. Taylor

SUMMARY: Well 163/6-1A, located in the northern part of the Rockall Trough, proved the presence of a thick sequence of extrusive igneous rocks below Upper Palaeocene sediments. K-Ar age dating suggests that the lavas were extruded at approximately 55 Ma. The lava sequence comprises three distinct lithologies. The upper part of the pile consists of olivine tholeiites that show alkalic and picritic tendencies and have a distinct within-plate composition. These are underlain by another group of olivine tholeiites that are much closer in composition to normal mid-ocean ridge basalt (N-type MORB). The Sr and Pb isotopic compositions of the basalts suggests possible contamination by continental crustal material.

The basalts are underlain by a sequence of cordierite-phyric dacites of remarkably homogeneous composition. Their highly aluminous nature, high Ni and Cr contents and their Sr and Pb isotopic compositions indicate that they are not differentiates of a basaltic parent magma, and are considered to have originated by melting of argillaceous and, possibly, arenaceous rocks at depth. Organic-rich black shale lithologies may have been involved.

The Rockall Trough is an area of deep water separating the relatively shallow Rockall Plateau from the main UK landmass (see Fig. 1). It is believed to have formed by a phase of rifting and abortive sea-floor spreading, in either the late Palaeozoic (Russell & Smythe 1977) or the mid-Cretaceous (Roberts *et al.* 1981). However, there are no mappable magnetic anomalies in the central and northern parts of the Trough, which suggests an alternative hypothesis, that over much of its area it is underlain by attenuated continental crust. It has also been suggested that late Cretaceous–early Tertiary oceanic crust may be present locally, for example around Rosemary Bank (Dietrich & Jones 1980). It has been proposed on the basis of seismic reflection profiling that the basin is filled with Mesozoic sediments and Palaeocene lavas, capped by Eocene and younger sediments (Roberts 1975; Naylor & Shannon 1982).

Well 163/6-1A is at present the only well to have investigated the deep geology of the Trough. It was drilled by the British Natural Oil Corporation (BNOC) on behalf of a consortium of 19 companies and the UK Department of Energy at 59°48.65'N, 8°57.95'W, in the centre of the Trough at its northern limit, just S of the Wyville–Thomson Ridge, in a water depth of 1374 m (Fig. 1). The site lies close to an igneous centre originally termed 'A' by Roberts *et al.* (1983), and subsequently named 'Darwin'. Igneous centre B of Roberts *et al.* and Rosemary Bank, known by dredging to consist of late Cretaceous or Tertiary basalt (Dietrich & Jones 1980), also lie close to the site (Fig. 1). A line drawing of a multichannel

seismic profile across the Darwin igneous centre is shown in Fig. 2, and a lithological summary of the 163/6-1A sequence is shown in Fig. 3. The well encountered 689 m of basalt underlying Upper Palaeocene to Recent sediments. Below the basalts, a further 356 m of dacites were drilled before the hole was abandoned. This paper documents the results of investigations into the petrography, geochemistry and radiometric age of the extrusive rocks recovered in the well.

Analytical methods

Following optical petrographical description, determinations of phase chemistry were made by electron microprobe (EM), using a Link Systems energy-dispersive X-ray analyzer attached to a Geoscan electron microprobe (at BGS Keyworth) and a similar ED system on a Microscan V (at Edinburgh University). Vesicle fills were identified optically and by X-ray diffraction (XRD). Samples for geochemistry were selected on a petrographic basis to minimize, as far as possible, the effects of alteration, by choosing those samples without extensive alteration and by avoiding highly amygdaloidal material.

Major and trace element analyses were carried out by X-ray fluorescence (XRF) at Edinburgh University and by MESA (Midland Earth Science Associates). Rare-earth element (REE) abundances were determined by neutron activation analysis (INAA) at the Imperial College Reactor Centre.

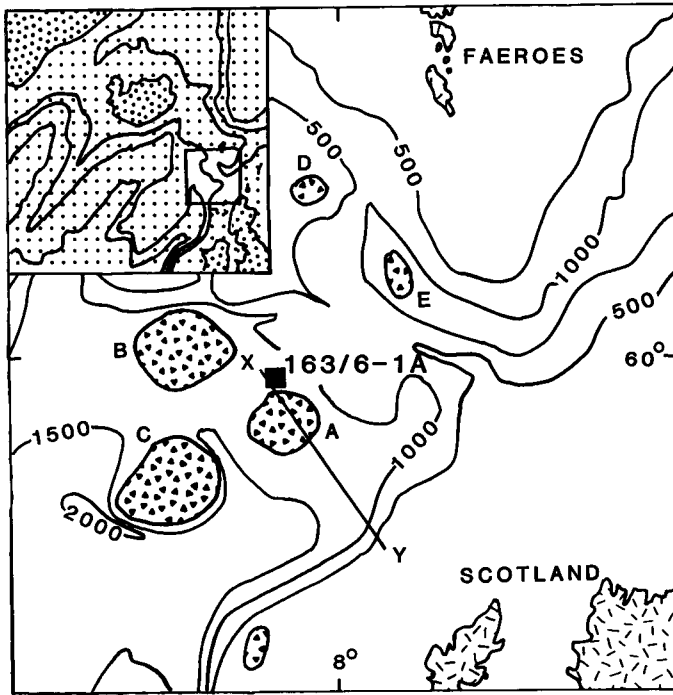


FIG. 1. Location of Well 163/6-1A and distribution of known and inferred igneous centres adjacent to the site. X-Y = line of seismic section shown in Fig. 2. A & B are igneous centres in northern Rockall Trough identified by Roberts *et al.* (1983). C: Rosemary Bank; D: Faeroe Bank Centre; and E: Faeroe Channel Knoll.

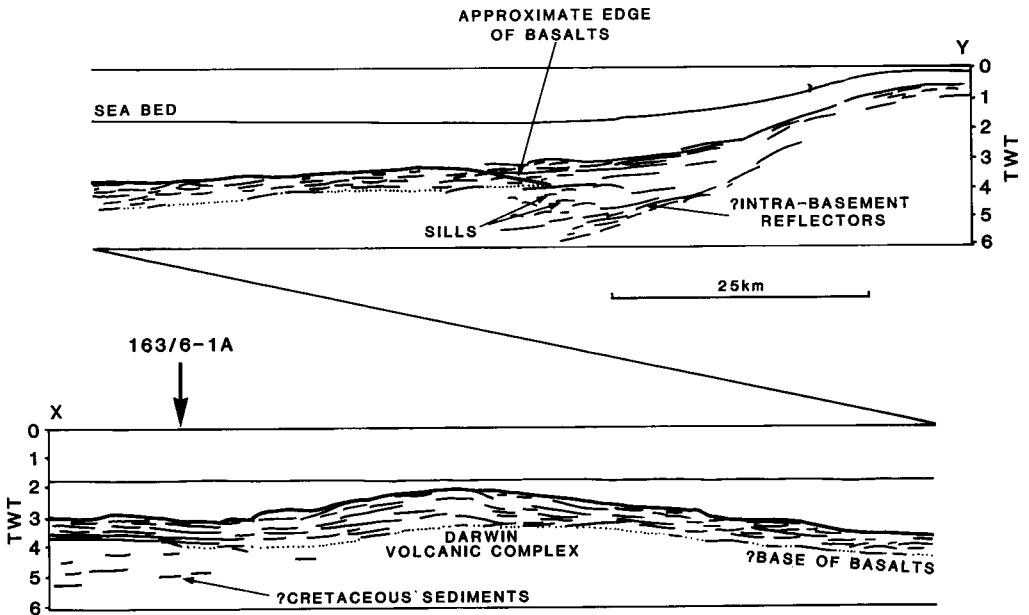


FIG. 2. Line drawing of multichannel line X-Y (Fig. 1) from the Hebridean shelf to 163/6-1A. The buried structural high of the Darwin volcanic complex is the volcanic centre A (Fig. 1) of Roberts *et al.* (1983). The basalts appear to be thin or absent near the edge of the trough, permitting acoustic penetration by a further 2-2.5 s (TWT). To the NW, the lack of reflectors below the presumed base of the basalts is due to insufficient transmission of energy through the basalts.

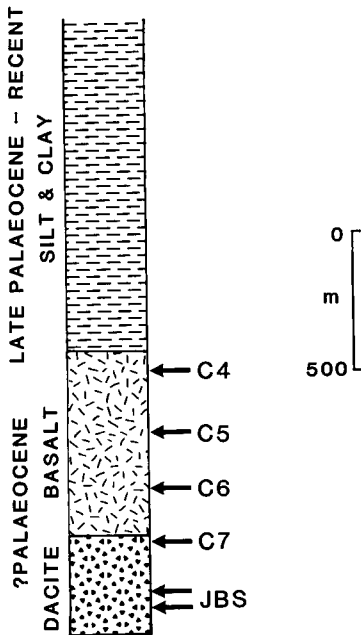


FIG. 3. Skeleton lithological log of sequence drilled in Well 163/6-1A, showing location of cores and junk basket samples.

Sr and Pb isotope geochemistry was carried out in the Department of Earth Sciences, University of Oxford. Sr samples were prepared by eluting Sr from cation exchange resin with 2.5 M HCl. $^{87}\text{Sr}/^{86}\text{Sr}$ ratios were determined both on whole-rock samples, and on sample residues after leaching in hot 6 M HCl. This procedure removes much of the Sr contained in alteration products, and was followed in an attempt to minimize the effects of any seawater alteration. Samples were loaded on single Ta filaments with H_3PO_4 and analyzed on a VG Micromass 30 thermal ionization mass spectrometer. Data were corrected for the effects of mass fractionation and for conformity with the inter-laboratory Eimer and Amend Sr standard ($^{87}\text{Sr}/^{86}\text{Sr} = 0.70800$).

Pb samples were prepared by loading the rock sample in 1 M HBr solution onto anion exchange resin, eluting Pb with pure H_2O . They were then loaded on single Re filaments with H_3PO_4 and silica gel activator, and were analyzed on a VG Isomass 54E fully automated thermal ionization mass spectrometer. Analyses were corrected for the effects of mass fractionation.

Whole-rock K-Ar dating was carried out at the Scottish Universities Research and Reactor Centre following procedures described by Macintyre & Hamilton (1984).

Basaltic rocks: petrography and chemistry

Three cores 4, 5 and 6, were taken in the basalt sequence.

Core 4

Core 4 (9.2 m long) contains four complete flow units, between 0.91 and 2.87 m thick, and two further partially cored flows, one at the top and one at the base of the core. The basalts are medium to fine-grained, dark grey to black and olivine-phyric. Individual flows have fine-grained, generally aphyric, highly vesicular tops, fine to medium-grained sparsely vesicular centres and fine-grained highly vesicular bases. No pillow structures or glassy rims were observed, and a subaerial origin is inferred.

The basalts of core 4 consist of olivine phenocrysts set in a groundmass of plagioclase laths, granular opaques, and pale to dark brown pyroxenes. The pyroxene is generally sub-ophitic, but in one sample (C4.5) it tends to be intersertal. This sample is from a flow top, unlike the others, which are from flow centres; the textural difference is therefore interpreted as the result of more rapid cooling.

Olivine contents lie between 18 and 40%. Except for one very olivine-rich sample (C4.1), in which the diameters of some olivines exceed 4 mm, the phenocrysts are generally small, around 0.5 mm. The large olivines are zoned from a core composition of Fo_{84-89} to a margin composition of Fo_{77-85} , whereas the smaller grains tend to be unzoned, with a composition of Fo_{71-85} . Several grains contain inclusions of dark brown magnesiochromite. Only two samples (C4.1 & C4.3) retain any fresh olivine; most are altered to smectite. Locally, an intermediate pale brown, low-birefringent alteration phase also occurs, shown by EM to be a serpentine-like mineral. In some cases, red-brown iddingsite is a further alteration product.

Plagioclase laths comprise between 30 and 50% of the rock. They are commonly zoned, from cores of An_{67-72} to rims as sodic as An_{26} . Plagioclase is mainly fresh, but some alteration to smectite and thomsonite has taken place.

Pyroxene contents lie between 13 and 23%. The dark colour is suggestive of a high TiO_2 content, confirmed by EM, which shows the pyroxenes to lie in the salite field (Fig. 4) and to have TiO_2 contents of 2.0–3.3%. This suggests that the basalts have an alkalic nature, although pyroxenes such as these are not uncommon in tholeiites. The pyroxenes plot in a relatively small

area on the $\text{TiO}_{2(\text{px})}$ - $\text{MnO}_{(\text{px})}$ - $\text{Na}_2\text{O}_{(\text{px})}$ diagram of Nisbet & Pearce (1976), mainly grouping in the 'within-plate alkalic' field (Fig. 5).

Opaques are a minor component, forming between 3 and 5% of the whole rock. Apart from one ilmenite-bearing sample (C4.1), the opaque phase is titanomagnetite.

The basalts also contain between 7 and 13% smectite as an alteration product of interstitial glass, none of which is preserved in a fresh state.

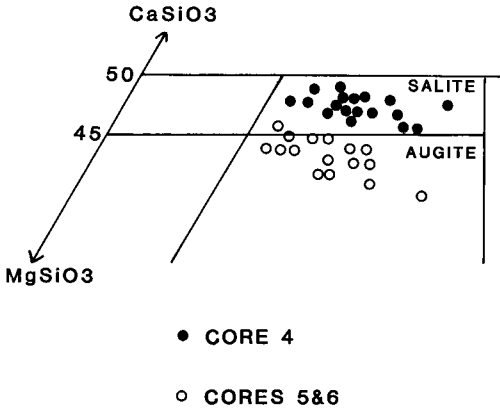


FIG. 4. Composition of clinopyroxenes in the basalts of 163/6-1A. Note the distinctly more calcic nature of the pyroxenes from core 4 (salites) compared to those of cores 5 and 6 (augites).

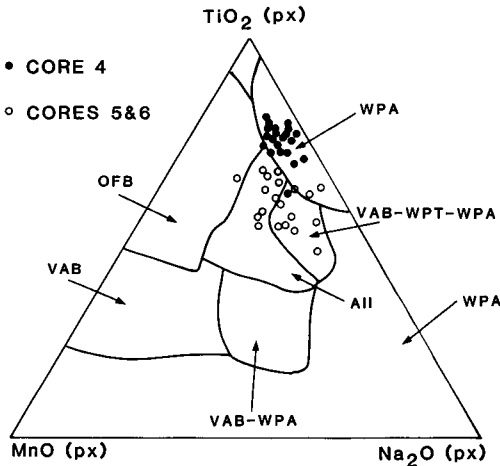


FIG. 5. Minor element geochemistry of clinopyroxenes from the basalts of 163/6-1A, plotted on the discrimination diagram formulated by Nisbet & Pearce (1976). Minor elements were determined by electron microprobe. WPA: within-plate alkali basalt; WPT: within-plate tholeiite; VAB: volcanic arc basalt; OFB: ocean floor basalt.

Areas of interstitial glass appear to have acted as nuclei for secondary clays, which also replace plagioclase and olivine.

Only one sample (C4.5) is markedly vesicular, being from a flow top. The vesicles are filled with spherulitic aggregates of smectite, bladed thomsonite, finely fibrous sheaf-like natrolite and weakly anisotropic analcime.

Apart from one picritic sample (C4.1) with an unusually high olivine content, there is comparatively little chemical variation between samples (Table 1). This is reflected by their CIPW norms, which show them to be olivine tholeiites, with one exception (C4.5). The normative nepheline of this sample is a result of secondary alteration, with an uptake of alkalis causing an excursion into the alkali basalt field.

Although the basalts have a tholeiitic nature, their alkalic tendencies are reflected in the presence of Ti-rich pyroxenes and high whole-rock Ti/V ratios (Shervais 1982), which fall in the narrow range 50–56 (Fig. 6). They show strong enrichment of Rb and Ba and moderate enrichment of K, Th, Sr, La, Ce, Nb, Ta and Nd relative to N-type MORB (Fig. 7). P, Hf, Zr, Eu

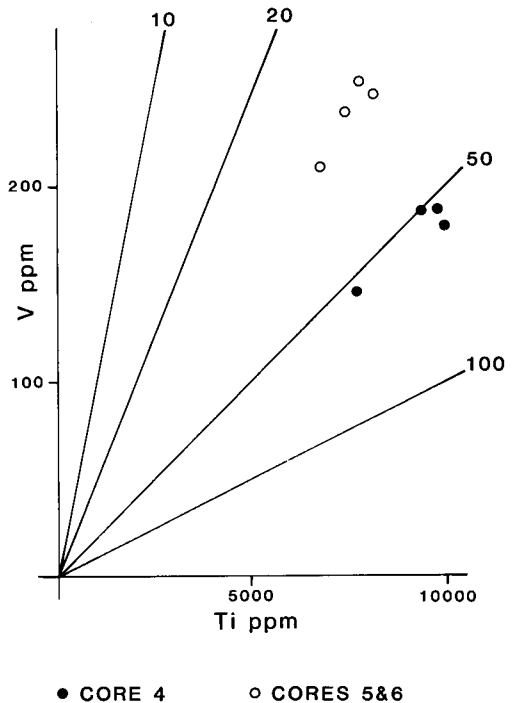


FIG. 6. Ti/V ratios of 163/6-1A basalts, plotted on the diagram devised by Shervais (1982). Increasing Ti/V reflects increasing alkalinity, Ti/V of 50 marking the distinction between mid-ocean ridge and continental flood basalts and alkali basalts.

TABLE 1. Geochemistry of basalts, core 4, Well 163/6-1A. Major and trace elements by XRF († by MESA, * at Edinburgh). Rare-earth elements by INAA at Imperial College Reactor Centre. Fe_2O_3/FeO ratios were fixed at 0.15 in normative calculations, following Brooks (1976)

Sample	C4.1†	C4.2*	C4.3†	C4.4†	C4.5*	C4.6*	C4.7†
SiO ₂	41.29	43.70	43.23	44.70	44.05	44.31	44.13
Al ₂ O ₃	9.48	13.04	12.65	14.29	14.81	14.66	14.08
TiO ₂	1.26	1.59	1.63	1.66	1.79	1.52	1.57
Fe ₂ O ₃	14.63	13.80	13.81	12.68	12.79	12.63	12.92
MgO	21.32	14.30	14.60	11.40	9.59	10.87	10.98
CaO	5.90	8.18	8.01	8.38	7.57	9.32	9.27
Na ₂ O	1.24	1.96	1.92	2.50	4.22	2.40	2.19
K ₂ O	0.07	0.13	0.10	0.16	0.22	0.16	0.15
MnO	0.19	0.17	0.18	0.16	0.16	0.16	0.16
P ₂ O ₅	0.10	0.13	0.13	0.18	0.18	0.15	0.17
LOI	4.72	3.30	3.91	4.10	4.60	3.70	4.41
Total	100.20	100.30	100.17	100.21	99.98	99.89	100.04
CIPW Norm							
Or	0.41	0.80	0.59	0.95	1.35	1.04	0.89
Ab	10.49	17.32	16.25	21.15	24.33	21.33	18.53
An	20.10	27.54	25.60	27.30	22.15	30.23	28.15
Ne					7.31		
Di	6.83	11.31	10.73	10.62	13.44	14.07	13.59
Hy	8.37	6.22	6.14	6.01		1.76	5.80
Ol	42.84	30.87	29.95	23.20	25.03	25.87	21.92
Mt	2.52	2.48	2.38	2.19	2.34	2.29	2.23
Il	2.39	3.15	3.10	3.15	3.61	3.03	2.98
Ap	0.24	0.30	0.31	0.43	0.45	0.39	0.40
Ba	96	59	55	95	69	86	125
Cr	963	812	925	480	451	651	610
Cu	44	42	44	26	60	18	18
Ni	943	492	516	396	249	405	442
Nb	5	6	5	5	8	7	6
Pb		5			7	6	
Rb	4	3	4	4	3	3	4
Sr	158	225	223	257	251	267	251
V	146	233	189	180	274	231	187
Y	14	16	19	21	20	18	21
Zn	82	86	77	81	85	80	72
Zr	77	83	90	111	117	98	114
La	3.7		4.7	6.2			6.2
Ce	9.0		13.5	17.8			17.2
Nd	8.1		11.1	13.2			14.0
Sm	2.29		3.04	3.70			3.69
Eu	0.80		1.11	1.35			1.31
Tb	0.41		0.55	0.62			0.59
Ho	0.31		0.55	0.54			0.52
Yb	0.66		0.91	1.08			1.11
Lu	0.12		0.16	0.20			0.20
Ta	0.20		0.27	0.38			0.35
Th	0.23		0.28	0.38			0.45
Hf	1.59		2.09	2.63			2.50

and Ti values are comparable to N-type MORB, but Tb, Y and Yb are increasingly depleted. According to Pearce (1982), the last feature is characteristic of within-plate basalts, whether they be tholeiitic, transitional or alkalic (fig. 1b,

Pearce 1982). They are relatively light rare-earth element (LREE)-enriched, with $(Ce/Yb)_N > 1$ (Fig. 7). A within-plate setting is also suggested by pyroxene chemistry (see Fig. 5), and is further demonstrated by the Pearce & Cann (1973) Ti-Y-

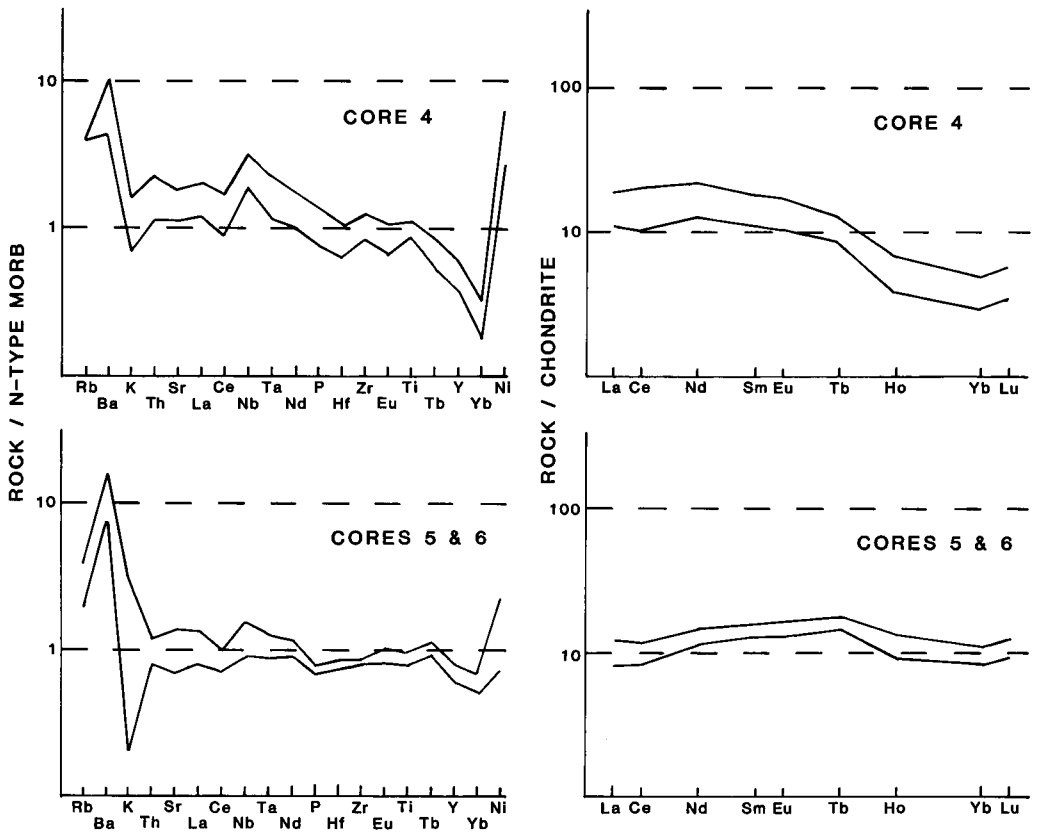


FIG. 7. Multi-element plots, normalized to N-type MORB, and chondrite-normalized rare-earth plots of basalts from 163/6-1A. Data shown are upper and lower limits of elemental abundances.

Zr diagram (Fig. 8). However, it should be emphasized that there are several known instances of MORBs plotting outside the ocean-floor basalt field on this diagram, such as mid-Atlantic Ridge basalts from DSDP Sites 407 and 408 (63°N) and 410 (45°N) (Tarney *et al.* 1979) and many Icelandic basalts (Prestvik 1982). On the Th-Ta-Hf diagram of Wood *et al.* (1979) they fall within the E-type MORB/WPB field, close to the transitional MORB area (Fig. 9).

Core 5

Core 5 (9.2 m long) recovered five flow units, three of which were complete, between 1.69 and 2.67 m thick. The basalts are fine to very fine-grained and sparsely plagioclase- and olivine-phyric. They are paler in colour than core 4 basalts, owing to their greater degree of alteration. The internal subdivisions of the flows are similar to those in core 4, although vesicles are more common in flow centres, and those in flow tops are commonly unfilled. The lack of pillow

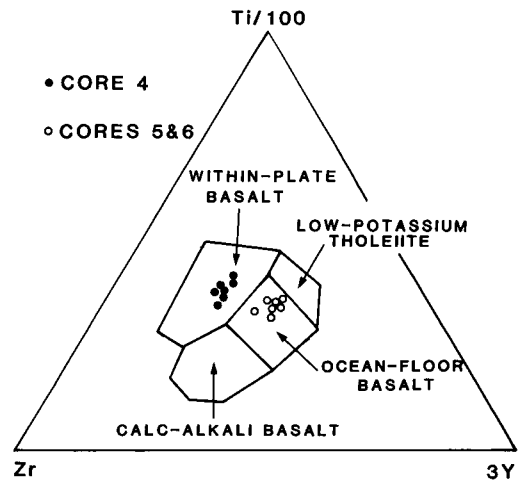


FIG. 8. 163/6-1A basalts plotted on the Ti-Y-Zr diagram of Pearce & Cann (1973).

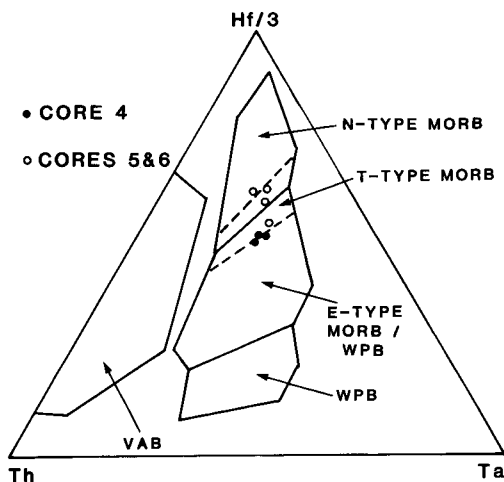


FIG. 9. 163/6-1A basalts plotted on the Th-Ta-Hf diagram of Wood *et al.* (1979).

structures and glassy rims again suggests a subaerial origin.

The basalts consist of plagioclase and olivine phenocrysts, in some cases with a glomerophytic habit, in a groundmass of plagioclase laths and granular pyroxene, with minor opaques tending to occur subpoikilitically.

Highly altered olivine occurs as scattered phenocrysts up to 2 mm in diameter and as microphenocrysts up to 0.1 mm long, and forms 8–9% of the rock. It is wholly replaced by serpentine and/or chlorite and smectite, precluding an assessment of original chemistry.

Plagioclase occurs both as a phenocryst and as a groundmass phase. Phenocryst plagioclase forms 10–12% of the rock, and plagioclase comprises a further 33–37% in the groundmass. In two samples (C5.1 & C5.2), both phenocryst and groundmass plagioclase have been wholly replaced by thomsonite, natrolite and K-feldspar. However, fresh plagioclase (An_{80-88} in the groundmass, phenocrysts zoned from cores of An_{82-86} to margins of about An_{52}) is preserved in samples C5.3 and C5.4.

Pyroxene is fresh throughout core 5. It occurs in colourless granules, and forms 20–24% of the rock. Compared to core 4, it is slightly less calcic (see Fig. 4), and is also poorer in TiO_2 (0.8–1.6%). Compared to those of core 4, core 5 pyroxenes plot in a different area on the Nisbet & Pearce (1976) $TiO_{2(pX)}-MnO_{(pX)}-Na_2O_{(pX)}$ diagram (see Fig. 5).

Opagues form 3–4% of the rock, and consist of titanomagnetite. Interstitial glass has been wholly replaced by smectite. Smectite, analcime, meso-

lite, natrolite, thomsonite and possible gonnardite occur as vesicle fills.

Although three out of the four samples studied (C5.1, C5.2 & C5.3) have normative nepheline (Table 2), the basalts of core 5 are clearly tholeiitic, the anomalous nepheline-normative character being an effect of alteration. Their tholeiitic nature is shown by their high Y/Nb ratios (5.3–8.7), their low Ti/V ratios (31–32, Fig. 6) and their flat patterns on MORB-normalized spidergrams (see Fig. 7). They therefore bear a strong resemblance to MORB, the only major departures being the high Rb and Ba and a slight tendency for Y and Yb depletion. However, both Rb and Ba are highly mobile elements during alteration and, furthermore, high Ba contents may be due to contamination by drilling mud. They have slightly convex-upward REE patterns (see Fig. 7), with $(Ce/Yb)_N$ close to 1, but relative enrichment of the middle REE Sm, Eu and Tb. They fall into the ocean-floor basalt field on the Pearce & Cann (1973) Ti-Y-Zr diagram (see Fig. 8). However, there are many cases of MORB-like basalts undoubtedly located within-plate, such as the Preshal Mhor and Fairy Bridge basalts of Skye and the low-alkali tholeiites of Mull (Morrison 1978). On the Th-Ta-Hf diagram of Wood *et al.* (1979) they fall in the transitional MORB field (Fig. 9).

Core 6

Core 6 (9.2 m recovered length) contains dark grey medium to fine grained olivine-microphyric basalts, somewhat fresher in appearance than those of core 5. Five flow units were recovered, three of which are complete, ranging in thickness from 0.10–1.01 m. Internal morphology of flows is again similar to that described for core 4, although flow centres are much reduced in thickness because of the relatively thin nature of the flows. Two of the flows have reddened tops, suggesting that extrusion took place subaerially.

The basalts consist of olivine microphenocrysts set in a groundmass of plagioclase laths and opaques, sub-ophitically enclosed by pyroxene. Compaction during crystallization has locally caused sub-ophitic pyroxene to fracture into a mosaic of subgrains which are out of optical continuity.

Olivine is entirely pseudomorphed by smectite and as with core 5 this precludes an assessment of its original composition. Olivine pseudomorphs comprise 11–19% of the rock.

Plagioclase occurs only as a groundmass phase, and is generally unaltered, although in one sample (C6.3) there is a significant proportion of smectite pseudomorphs after plagioclase laths. Plagioclase

TABLE 2. *Geochemistry of basalts, core 5, Well 163/6-1A. Major and trace elements by XRF († by MESA, * at Edinburgh). Rare-earth elements by INAA at Imperial College Reactor Centre. Fe₂O₃/FeO ratios were fixed at 0.15 in normative calculations, following Brooks (1976)*

Sample	C5.1†	C5.2*	C5.3*	C5.4†
SiO ₂	45.75	44.46	45.04	45.18
Al ₂ O ₃	14.10	15.14	15.81	14.22
TiO ₂	1.30	1.21	1.27	1.13
Fe ₂ O ₃	12.47	11.92	12.20	11.88
MgO	8.79	8.15	8.53	11.90
CaO	7.56	8.81	10.98	10.56
Na ₂ O	4.76	4.23	2.76	1.59
K ₂ O	0.30	0.24	0.13	0.02
MnO	0.19	0.17	0.14	0.20
P ₂ O ₅	0.10	0.08	0.08	0.09
LOI	5.01	6.30	3.40	3.58
Total	100.33	100.71	100.34	100.37

CIPW Norm

Or	1.77	1.52	0.76	0.12
Ab	25.49	22.57	19.90	13.45
An	16.22	23.16	31.66	31.61
Ne	7.11	8.54	2.43	
Di	16.87	18.89	20.15	16.35
Hy				12.55
Ol	21.01	20.46	20.20	17.25
Mt	2.15	2.20	2.19	2.04
Il	2.47	2.45	2.51	2.15
Ap	0.24	0.21	0.20	0.21
Ba	146	162	66	103
Cr	268	268	272	550
Cu	145	101	112	105
Ni	106	98	100	321
Nb	3	3	3	4
Pb		7	8	
Rb	4	4	2	2
Sr	95	207	162	119
V	253	326	327	210
Y	26	23	24	21
Zn	63	76	74	71
Zr	72	57	60	71
La	2.7			4.0
Ce	7.3			10.1
Nd	7.3			8.5
Sm	2.64			2.98
Eu	1.01			1.13
Tb	0.71			0.69
Ho	0.82			0.72
Yb	1.94			1.84
Lu	0.32			0.32
Ta	0.16			0.35
Th	0.18			0.16
Hf	1.85			2.16

originally formed 39–47% of the rock, and is zoned from An_{73–83} in grain centres to margins of An₃₆.

Pyroxene forms 21–32% of the basalts and, in compositional terms, it is similar to that of core 5 and distinct from that of core 4 (see Figs 4 & 5).

Opaques are minor constituents, forming 4–5% of the rock, and consist of titanomagnetite, ilmenite and chromite.

The lower degree of alteration in core 6 means that the CIPW norms are a better guide to character than they were in core 5, with only one sample (C6.3) being anomalously nepheline-normative (Table 3). Their tholeiitic character is confirmed by their high Y/Nb and low Ti/V ratios, by their flat patterns on MORB-normalized spidergrams (see Fig. 7) and by their REE patterns (see Fig. 7). The close similarity of basalts from cores 5 and 6 is also shown on Ti/V (see Fig. 6), Ti-Y-Zr (see Fig. 8) and Th-Ta-Hf (see Fig. 9) diagrams.

Dacitic rocks: petrography and chemistry

Black, very fine-grained cordierite-phyric dacites were recovered in core 7. Large, filled vesicles are sparsely distributed throughout the cored interval. No textural trends were noted, implying that the core (3.2 m long) was taken from within a single flow unit. Two junk basket samples from lower in the succession also consist exclusively of dacite, in variable states of alteration. Black, glassy and apparently relatively fresh material occurs in both, as well as more altered, greenish-grey fine-grained pieces, several of which are sparsely vesicular and traversed by abundant fine veins. One junk basket sample also contains light grey, fine-grained, relatively fresh pieces.

Petrographic study shows that, despite variations in degree of crystallinity and alteration, the dacitic sequence is remarkably homogeneous. All samples contain abundant cordierite phenocrysts or pseudomorphs after cordierite, together forming between 11 and 24% of the rock. The groundmass is generally microcrystalline, but is glassy in sample JB2B, indicating rapid quenching. In the core, cordierite is entirely replaced by yellow-green chlorite, but is fresh in some pieces from the junk basket samples. The cordierite is moderately iron-rich and occurs as euhedral short hexagonal prisms up to 0.5 mm long, often in glomerophyric aggregates. Basal sections show the characteristic sector twinning. Many contain inclusions of rounded bytownite (An₈₁). One sample (JB2A) also contains phenocrysts of

TABLE 3. *Geochemistry of basalts, core 6, Well 163/6-1A. Major and trace elements by XRF († by MESA, * at Edinburgh). Rare-earth elements by INAA at Imperial College Reactor Centre. Fe₂O₃/FeO ratios were fixed at 0.15 in normative calculations, following Brooks (1976)*

Sample	C6.1†	C6.2*	C6.3†	C6.4*
SiO ₂	46.42	46.16	46.94	45.37
Al ₂ O ₃	15.14	15.34	14.02	14.77
TiO ₂	1.24	1.14	1.36	1.13
Fe ₂ O ₃	12.82	12.03	13.20	11.65
MgO	8.14	9.85	7.76	11.49
CaO	12.37	11.74	10.54	10.84
Na ₂ O	1.98	2.24	3.54	1.79
K ₂ O	0.07	0.06	0.08	0.05
MnO	0.19	0.20	0.18	0.19
P ₂ O ₅	0.09	0.07	0.10	0.08
LOI	1.57	2.20	2.37	3.20
Total	100.02	101.01	100.08	100.56
CIPW Norm				
Or	0.41	0.34	0.47	0.29
Ab	16.75	19.41	24.49	15.63
An	32.22	32.36	22.13	32.36
Ne			2.63	
Di	23.43	21.81	24.26	17.70
Hy	6.80	0.06		8.63
Ol	12.93	21.53	17.16	19.82
Mt	2.20	2.12	2.28	2.08
Il	2.35	2.20	2.58	2.24
Ap	0.21	0.17	0.24	0.20
Ba	198	26	142	27
Cr	394	440	233	650
Cu	69	85	130	88
Ni	225	204	112	302
Nb	3	4		3
Pb		8		8
Rb	3	2	2	1
Sr	145	133	188	127
V	238	301	247	282
Y	27	22	28	20
Zn	59	68	65	77
Zr	77	60	71	61
La	3.6		2.4	
Ce	9.7		9.1	
Nd	9.1		9.5	
Sm	3.20		3.23	
Eu	1.20		1.29	
Tb	0.73		0.83	
Ho	1.02		1.04	
Yb	2.02		2.17	
Lu	0.35		0.43	
Ta	0.15		0.16	
Th	0.24		0.24	
Hf	2.13		1.89	

magnesian hypersthene, again forming glomerophytic aggregates.

Groundmass phases include very fine-grained labradorite and sanidine (EM has detected plagioclase of An₅₈ and K-feldspar of Or₅₆) and opaques. Vesicles are filled with smectite, several zeolites (including natrolite, heulandite and morденite), cristobalite and opaques.

Geochemical studies confirm the homogeneous nature of the dacitic sequence (Table 4). The dacites are remarkable for their high Al content, manifested by the 6% normative corundum and by the abundant cordierite phenocrysts. Ni, Cr and, to a lesser extent, V are remarkably high for such siliceous rocks. Relative to chondrite, they show strong LREE enrichment (Fig. 10), and display a marked negative Eu anomaly. Fig. 10 also includes a MORB-normalized spidergram, emphasizing the strong geochemical differences between these dacites and the overlying basalts.

Isotope geochemistry

Sr isotopes

Initial ⁸⁷Sr/⁸⁶Sr ratios of seven samples (five basalts, two dacites) are presented in Table 5. Three basalt samples (C4.1, C4.2, C5.4) have very low initial ⁸⁷Sr/⁸⁶Sr ratios (0.70313–0.70329, reduced to 0.70298–0.70317 after acid leaching), typical of mid-Atlantic Ridge basalts. However, the other two samples analyzed (C5.1 & C6.3) have significantly higher initial ⁸⁷Sr/⁸⁶Sr ratios of 0.70392–0.70435 (0.70398–0.70457 after acid treatment). These values are above the range for typical MORB, although not beyond the range for basalts derived from mantle sources less depleted than MORB-source mantle. However, these samples have MORB-like chemistry, tending to rule out the latter possibility. The implication, therefore, is that samples C5.1 and C6.3 have been slightly contaminated by continental crustal material. Both dacite samples have very high initial ⁸⁷Sr/⁸⁶Sr ratios (0.71102–0.71112), and it is notable that acid leaching has the effect of increasing ⁸⁷Sr/⁸⁶Sr in the residue to 0.71211–0.71216. This suggests that leaching has removed Sr held in alteration products, probably Sr substantially modified in isotopic composition by interaction with seawater Sr, which had an ⁸⁷Sr/⁸⁶Sr ratio of about 0.7077 in the early Tertiary (Burke *et al.* 1982). These values are well outside the range of MORB, clearly indicating that material of continental derivation has played an important role in the genesis of the dacites.

TABLE 4. *Geochemistry of dacites, Well 163/6-1A. Major and trace elements by XRF († by MESA, * at Edinburgh). Rare-earth elements by INAA at Imperial College Reactor Centre. Fe₂O₃/FeO ratios were fixed at 0.15 in normative calculations, following Brooks (1976)*

Sample	C7.1†	C7.2†	JB1A*	JB1B*	JB2A*	JB2B*
SiO ₂	64.48	64.52	62.92	67.61	61.63	63.53
Al ₂ O ₃	16.14	16.08	16.28	15.11	17.11	15.79
TiO ₂	0.92	0.90	0.91	0.83	0.95	0.87
Fe ₂ O ₃	6.55	6.70	5.41	2.60	6.26	5.54
MgO	1.77	1.53	1.95	0.82	2.03	1.90
CaO	2.51	2.22	2.57	2.04	2.58	2.65
Na ₂ O	2.06	2.12	1.25	1.08	1.26	2.13
K ₂ O	2.63	2.57	2.57	2.04	2.58	2.65
MnO	0.11	0.14	0.09	0.05	0.13	0.12
P ₂ O ₅	0.17	0.16	0.17	0.15	0.15	0.15
LOI	2.99	3.23	4.50	3.30	4.50	5.80
Total	100.34	100.16	99.84	100.06	100.29	99.52
CIPW Norm						
Qz	31.45	32.18	32.15	31.44	30.31	38.87
Co	5.75	6.16	6.19	3.06	7.08	7.22
Or	15.54	15.19	23.61	39.61	22.85	6.55
Ab	17.43	17.94	11.14	9.49	11.17	19.31
An	11.34	9.97	12.22	9.50	12.36	13.00
Hy	11.98	11.67	11.44	4.43	12.80	11.86
Mt	1.13	1.16	0.98	0.46	1.13	1.02
Il	1.75	1.71	1.82	1.64	1.91	1.76
Ap	0.40	0.38	0.44	0.36	0.39	0.39
Ba	588	712	297	492	133	272
Cr	135	97	202	129	149	157
Cu	18	20	16	15	15	14
Ni	55	46	77	43	58	63
Nb	18	16	17	16	19	17
Pb			20	18	18	21
Rb	96	96	93	114	82	89
Sr	149	149	118	119	122	257
Th			17	14	16	13
V	123	127	159	144	163	150
Y	34	35	31	27	33	30
Zn	89	87	93	76	82	101
Zr	207	207	213	200	229	206
La	40.8	40.8				
Ce	96	98				
Nd	41.4	43.9				
Sm	7.80	8.02				
Eu	1.46	1.48				
Tb	1.00	1.03				
Ho	1.41	1.49				
Yb	3.06	3.01				
Lu	0.55	0.54				
Ta	1.32	1.21				
Th	12.7	13.1				
U	2.54	2.23				
Hf	6.16	6.61				

Pb isotopes

Pb-isotopic data are presented in Table 6 and shown on a $^{207}\text{Pb}/^{204}\text{Pb}$ - $^{206}\text{Pb}/^{204}\text{Pb}$ diagram

(Fig. 11). Also shown on this diagram is the area in which typical MORB falls (from Gariépy *et al.* 1983), the Pb-isotopic compositions of the Faeroes Upper Series basalts, also from Gariépy *et al.*

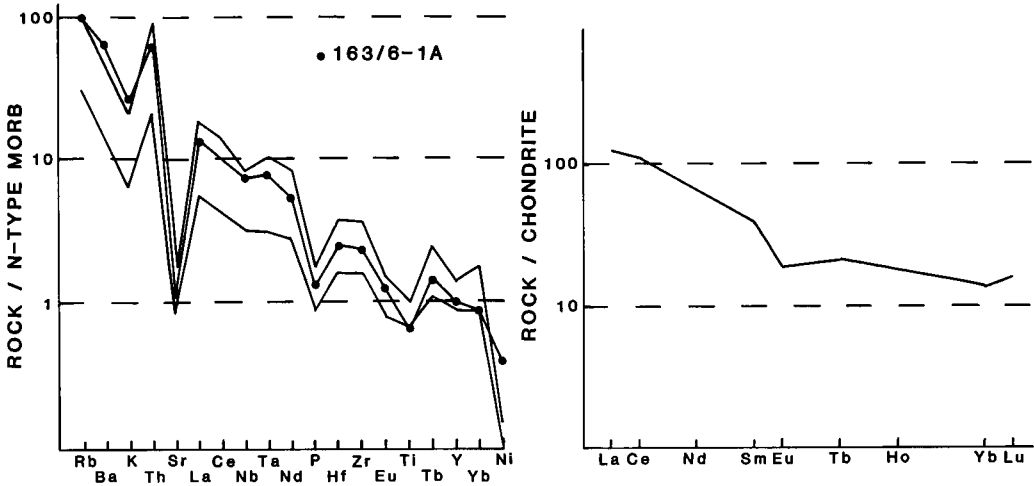


FIG. 10. MORB-normalized spidergram and chondrite-normalized rare-earth plot of 163/6-1A dacites. Also shown on MORB-normalized spidergram is the range of Lower Series peraluminous rocks recovered at Site 642 of the Ocean Drilling Programme on the Vøring Plateau, Norwegian Sea (Eldholm *et al.* 1987).

TABLE 5. *Sr-isotopic characteristics of basalts and dacites, Well 163/6-1A. Initial ratios calculated assuming 55 My in situ Rb decay. Initial ratios for leached samples are approximate, corrected from present compositions using whole-rock Rb/Sr ratios*

Sample	Present		Initial	
	⁸⁷ Sr/ ⁸⁶ Sr unleached	⁸⁷ Sr/ ⁸⁶ Sr leached	⁸⁷ Sr/ ⁸⁶ Sr unleached	⁸⁷ Sr/ ⁸⁶ Sr leached
C4.1	0.70335 ± 3	0.70316 ± 4	0.70329	0.70310
C4.2	0.70330 ± 6	0.70321 ± 6	0.70326	0.70317
C5.1	0.70445 ± 5	0.70467 ± 5	0.70435	0.70457
C5.4	0.70317 ± 6	0.70302 ± 5	0.70313	0.70298
C6.3	0.70394 ± 5	0.70400 ± 5	0.70392	0.70398
C7.1	0.71258 ± 6	0.71362 ± 5	0.71112	0.71216
C7.2	0.71248 ± 5	0.71356 ± 4	0.71102	0.71211

TABLE 6. *Pb-isotopic characteristics of basalts and dacites, Well 163/6-1A*

Sample	²⁰⁶ Pb/ ²⁰⁴ Pb	²⁰⁷ Pb/ ²⁰⁴ Pb	²⁰⁸ Pb/ ²⁰⁴ Pb
C4.1	18.34	15.55	38.25
C4.2	18.37	15.54	38.25
C5.4	18.18	15.57	38.07
C6.3	17.77	15.56	37.58
C7.1	18.54	15.58	38.60
C7.2	18.57	15.63	38.75

al. (1983), and the lines representing hypothetical 'orogene' and 'upper crust' source compositions, from Zartman & Doe (1981). The Faeroes Upper Series are included because their Pb-isotopic compositions have been modified by contamination with ancient continental basement, because they are closely contemporaneous with the 163/6-1A basalts, and have comparable chemistry, and because 163/6-1A is comparatively close to the Faeroes.

On this diagram, the 163/6-1A basalts fall on the top edge of the MORB field, or slightly above it, and the dacites similarly fall above the MORB field, close to the hypothetical 'orogene' line of Zartman & Doe (1981). This implies that the dacites have initial Pb-isotope characteristics similar to those predicted for magmas derived from mixed crust-mantle sources, and that their isotopic composition is dominated by material from the upper continental crust. The basalts also appear to have been contaminated by upper crustal material. Therefore, the 163/6-1A lavas have interacted with crust of a different nature to that which has contaminated the Faeroes basalts. The effect shown by the Faeroes Upper Series is for deviation from typical MORB toward a single unradiogenic sample with ²⁰⁷Pb/²⁰⁴Pb = 15.184 and ²⁰⁶Pb/²⁰⁴Pb = 16.100. Contamination of this type is considered to be due to interaction with ancient U-depleted material typical of the lower crust.

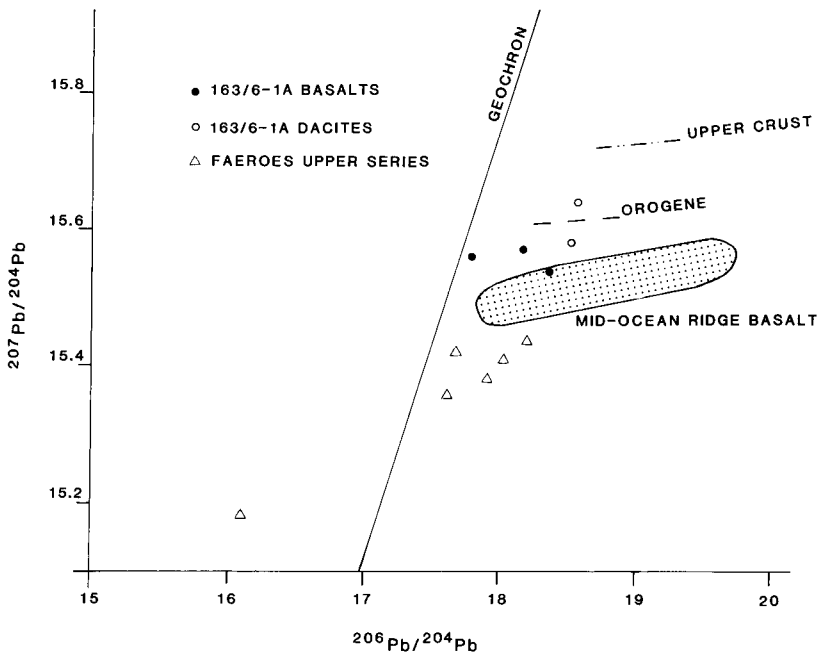


FIG. 11. Pb-isotopic composition of 163/6-1A basalts and dacites, with range of MORB and Faeroes Upper Series basalts (from Gariepy *et al.* 1983) shown for comparison.

K-Ar age measurements

K-Ar ages were determined on six whole-rock samples of basalt and four of dacite. The results of these measurements are presented in Table 7. The ages have been computed in the conventional manner on the assumption that all of the non-radiogenic argon measured in an analysis has an isotopic composition identical to that of modern atmospheric argon. Cores 4 and 5 have low but similar potassium contents, but core 6 is extremely K-deficient. The results of these flame-photometric analyses are in general agreement with those obtained by XRF, demonstrating the efficacy of this technique for K determination even at low levels. However, the results obtained on the junk basket samples are markedly dissimilar, presumably reflecting differences in composition of the subsamples analyzed. As a result of the low potassium contents and relative youthfulness of the basalts, the analytical uncertainty in their age measurements is quite high. Additionally, the extraction and purification of the radiogenic argon from some samples was hampered by the presence of hydrocarbons and, as some of these occur in the same region of the mass spectrum as the argon isotopes, they are potential interferants during mass spectrometric analysis and could lead to computation of misleading results. This

TABLE 7. K-Ar data, basalts and dacites, Well 163/6-1A

Sample	K wt %	$^{40}\text{Ar}^*$ ($\times 10^{-7}$ scc/g)	$^{40}\text{Ar}^*/^{40}\text{Ar}_T$	Age (Ma)
Basalts				
C4.2	0.100	2.10	9.02	53 ± 7
		3.42	18.5	(86 ± 6)
C4.6	0.143	3.10	21.5	55 ± 3
C5.2	0.195	4.48	30.2	58 ± 2
C5.3	0.105	2.38	24.8	57 ± 3
C6.2	0.063	1.41	14.9	57 ± 5
		1.93	22.6	(77 ± 4)
Dacites				
C6.3	0.050	1.61	12.1	(81 ± 8)
C7.3	2.19	43.84	88.2	50.9 ± 1.0
C7.4	2.10	46.52	88.0	56.2 ± 1.2
		45.2	69.6	54.6 ± 1.3
JB2A	4.39	133.7	29.9	77 ± 3
		122.1	42.2	70 ± 2
JB2B	0.921	243.6	32.4	580 ± 20
		318.8	42.6	720 ± 20

$^{40}\text{Ar}^*$: radiogenic ^{40}Ar ; $^{40}\text{Ar}_T$: total ^{40}Ar ; λ_β : 4.962×10^{-10} yr; λ_e : 0.581×10^{-10} yr; ^{40}K : 1.167×10^{-2} atom %; errors computed from $(E_K^2 + (1+A/R)^2 E_{40}^2 + E_{38}^2 + (A/R)^2 E_{36}^2)^{1/2}$, where $R = (100 - A) = ^{40}\text{Ar}^*/^{40}\text{Ar}_T$ with error in K, $E_K = 1.5\%$ and errors in peak heights, $E_{40} = E_{38} = 0.5\%$, $E_{36} = 1\%$.

potential problem was recognized at an early stage and careful checks were carried out on all subsequent samples undergoing analysis. No evidence was found for the presence of any hydrocarbons following gas purification and it is not considered that the measured ages are, therefore, uncertain.

For the purposes of discussion, the results in Table 7 are best considered in two groups. The first group consists of all the analyzed basaltic rocks (C4.2, C4.6, C5.2, C5.3, C6.2 & C6.4) and two dacites (C7.3 & C7.4). With three exceptions, most of the apparent ages of this group lie in the restricted range 51–58 Ma, and average 55 Ma. This is probably close to the age of the lavas, as all samples but one (C7.3) fall within analytical error of this. Weathering and alteration can facilitate argon loss, lowering the measured ages. Unfortunately, the least altered samples from core 6 are extremely K-deficient. There does not appear to be any significant difference in age between the dacites and the basalts, a finding which is of significance in their genesis.

The second group comprises the junk basket samples JB2A and JB2B, both of which were analyzed twice. JB2A gave apparent ages of 70 Ma and 77 Ma, and JB2B gave apparent ages of 580 Ma and 720 Ma. Although a late Cretaceous date for the lower part of the dacite sequence is not unreasonable, the apparent age of JB2B is clearly anomalous. Approximately 93% of the measured ^{40}Ar in this sample could not have been derived radiogenically by the *in situ* decay of ^{40}K since the late Cretaceous–early Tertiary. This suggests that JB2A similarly contains extraneous argon.

Both of these samples are distinctive in containing a high proportion of cordierite phenocrysts, many of which are fresh. It has been known for some time that this mineral can host excess argon (Damon & Kulp 1958), located in the wide channels in the crystal structure where it is trapped by cationic 'blocks'. The concentration of extraneous ^{40}Ar in the cordierite of JB2 (ca. 1.3×10^{-4} scc/g) falls in the middle of the range already observed for this mineral (York *et al.* 1969; York & Farquhar 1972, pp. 53–56). JB2B has a glassy groundmass, indicative of rapid chilling. Although it is unlikely that extrusion took place under high hydrostatic pressure, in view of the subaerial nature of the nearby Faeroes lava pile and the presence of reddened tops to basalt flows in core 6, the chilling may have effectively sealed a sample of magmatic gas, packaging and preserving it for posterity. In JB2A, the more microcrystalline nature of the groundmass may have allowed the release of some of the trapped argon; in this

instance, the effect on the apparent age is less marked because of the higher potassium content. In the core samples, where the cordierite has been replaced by chlorite, argon release seems to have been complete.

Both the junk basket dacites have high ^{36}Ar contents (up to 3×10^{-7} scc/g). Consequently, sea water must have played a role in the genesis of these rocks, as this is the only reservoir capable of supplying ^{36}Ar in such concentrations (see Allègre *et al.* 1987, table 1). This conclusion is consistent with the increase in $^{87}\text{Sr}/^{86}\text{Sr}$ found during acid leaching. This involvement with sea water suggests that the ^{40}Ar excesses found in these rocks could have been derived through the interaction and/or assimilation of older sediments bearing K-rich detritus, which had not been completely degassed on diagenesis. This is similar to the origin proposed for excess argon in the contemporaneous lavas from DSDP Sites 553 and 555 (Macintyre & Hamilton 1984). These lavas have extraneous gas with similar $^{40}\text{Ar}/^{36}\text{Ar}$ ratios (ca. 440), but this may be fortuitous as the gas analyzed from Well 163/6-1A may be an admixture of sea water (295) and magmatic (>440) components. The presence of hydrocarbons in the sequence suggests that the sediments that were involved may have been organic in nature.

Discussion

The volcanic sequence in Well 163/6-1A consists of olivine tholeiites overlying cordierite-hypersthene dacites. The basalts may be divided into two groups on geochemical grounds, those of core 4 being significantly different from those of cores 5 and 6. The lower group have distinct MORB-like tendencies, with flat patterns on MORB-normalized spidergrams (see Fig. 7). They plot in the ocean-floor basalt field on the Ti-Y-Zr diagram (see Fig. 8) and in the transitional MORB field on the Ta-Th-Hf diagram (see Fig. 9). However, their pyroxene compositions suggest a within-plate origin (see Fig. 5). The upper basalts, although also olivine tholeiites, are distinctly more alkaline, with higher Ti/V and Nb/Y ratios. They show strong depletion of Y and Yb relative to N-type MORB (see Fig. 7), a feature typical of within-plate basalts (Pearce 1982), and fall into the within-plate basalt field on the Ti-Y-Zr diagram (see Fig. 8). Sr- and Pb-isotope studies suggest that upper continental crustal material has played a minor but significant role in the genesis of both basalt types. Both basalt types have parallels in the British Tertiary Volcanic Province. The basalts of core 4 have

REE patterns comparable to those of the Mull Plateau Group (Morrison *et al.* 1980) and to those of the Lower Basalt Formation of Antrim (Lyle 1985), whereas the basalts of cores 5 and 6 compare well with the Upper Basalt Formation of Antrim (Lyle 1985) and basalts of Preshal Mhor type in Skye (Thompson *et al.* 1980).

The two basalt types have similar highly incompatible element ratios. Mean La/Ta and La/Th values are 17.5 and 15.8 respectively for core 4 basalts, and 16.8 and 16.3 respectively for cores 5 and 6 basalts, although there is greater scatter associated with the ratios from basalts of cores 5 and 6, presumably related to lower analytical precision at the lower elemental abundances associated with this basalt type. Given this, the similarity in La/Ta and La/Th indicates that the same mantle source, under different partial melting conditions, could have been responsible for both magma types. This possibility is explored further in Fig. 12, a chondrite-normalized plot of Ce content against Ce/Yb ratio, as discussed by Saunders (1984). This shows that the basalts of cores 5 and 6 could be produced by high degrees of dynamic partial melting of a source with $(Ce)_{CN}=1.5$ and $(Ce/Yb)_{CN}=0.8$, and that those of core 4 could be generated by a lower degree of partial melt of the same source. The displacement of the core 4 basalts to the left of the dynamic melting curve can be interpreted to be the result of the abundant olivine phenocryst population; the sample with the maximum displacement from the curve is C4.1, the most olivine-rich of this group, with 40% modal olivine.

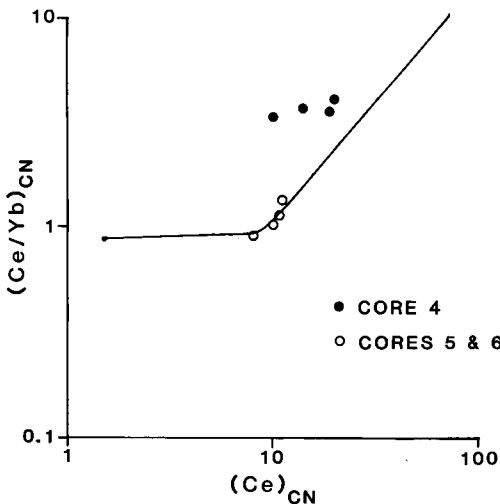


FIG. 12. 163/6-1A basalts plotted on a log-log plot of $(Ce/Yb)_{CN}$ ratio vs $(Ce)_{CN}$ content. Also shown is the dynamic melting curve of a garnet lherzolite source, from Saunders (1984).

Thus, the lower basalts at 163/6-1A appear to represent an early, large-scale melting event, with the succeeding basalts generated by lower degrees of melting as the heat source waned.

The dacites have an unusual chemistry and clearly represent a very specific petrogenetic process. Their corundum-normative character, abundant cordierite phenocrysts and high Ni and Cr contents all argue strongly against an origin by differentiation of an olivine tholeiite parent, which supplied the spatially associated basalts, and suggest that they were either generated by assimilation of argillaceous material or by extensive melting of a quartzo-feldspathic and argillaceous parent.

The dacitic magma has a melting point in excess of 1100° at 1 atm. The total assimilation of aluminous material by a dacitic parent magma would require an extraordinarily high initial magma temperature. Consequently, the melting hypothesis is preferred. In this model, shales, and possibly also sandstones, were in contact with a large body of high-temperature magma for a long period at depth. Their Pb- and Sr-isotopic compositions and high extraneous argon contents are consistent with such a petrogenetic model. Ponding of a large body of high-temperature basaltic magma within a sedimentary pile might be expected to allow the development of anatectic melts. Mixing of such anatectic melts with the basaltic magma may be strongly inhibited by a combination of the density contrast between melts and magma chamber geometry. For example, a pond of anatectic melt lying above basaltic magma could develop in a sheet-like magma chamber, where heat loss takes place almost entirely through the roof, or in a chamber with side walls inclined inwards toward the roof, so that low-density anatectic melts developed on the side walls are constrained to migrate upward along the side walls rather than through the basaltic magma. The development of large volumes of anatectic melt would require a very large heat input which could only be provided by the fractional crystallization of a very large volume of basaltic magma, presumably developing a large pile of cumulate gabbros. Because of the considerable amount of dacitic material produced (in excess of 350 m at the well site, although the lateral extent of the body is unknown), the magma chamber that acted as the heat source must have been large. The most likely location is the large igneous centre detected close by (see Fig. 1).

Some further inferences regarding the nature of the source material may be made from the geochemistry of the dacites. Of particular interest are the high Ni and Cr contents, because these

trace elements, along with V, Co, Cu and Zn, are enriched in organic black shale facies (Vine & Toutelot 1970; Cunningham & Gilbert 1984). There is, therefore, a strong possibility that black shales were included in the melt. If this is so, it seems likely that they were of Cretaceous age, as early Cretaceous black shales have been drilled in the Bay of Biscay and Goban Spur areas to the S of the Rockall Trough during DSDP Legs 48 and 80 (Timofeev & Bogolyubova 1979; Graciansky *et al.* 1979; Cunningham & Gilbert 1984). The postulated presence of a thick sedimentary sequence including excellent petroleum source rocks, such as black shales, has significant implications for the petroleum prospects of the Rockall Trough. In this context, it is noteworthy that the basalt sequence on the Faeroes contains migrated hydrocarbons (Waagstein *et al.* 1984), and also that hydrocarbons were detected in the volcanic sequence of the well in question here.

Prior to the drilling of the 163/6-1A dacites, peraluminous rocks were unknown from the NE Atlantic Igneous Province. It is, therefore, remarkable that similar rocks have recently been drilled at Site 642 on the Vøring Plateau (Norwegian Sea) during Leg 104 of the Ocean Drilling Programme. The sequence drilled at Site 642 comprises MORB-like tholeiites that form the dipping reflector sequence, overlying more silicic rocks, including cordierite-, hypersthene- and bytownite-phyric rocks (Eldholm *et al.* 1987).

These have remarkably similar trace element contents to the 163/6-1A dacites (see Fig. 10), and their initial $^{87}\text{Sr}/^{86}\text{Sr}$ ratios of 0.7115–0.7118 compare closely with the 0.7121–0.7122 values from the 163/6-1A dacites. These two discoveries, although spatially separated, are in broadly comparable tectonic settings and both are located close to the continental margin of the European landmass. Thus, although peraluminous extrusive and intrusive rocks in the NE Atlantic Igneous Province remained undiscovered until 1980, they appear to form an important part of the province, and may prove to be particularly significant in a tectonic context.

ACKNOWLEDGEMENTS: The cooperation of many individuals and groups was required in this study, and thanks are due to all involved. Britoil kindly provided junk basket samples to supplement the core study. Dr B Atkin (MESA) and Mrs D James (Edinburgh) organized the XRF analyses, and Dr I Sinclair and Dr S Parry (Imperial College) carried out the neutron activation analyses. The Isotope Geology Unit at SURRC receives financial support from NERC and the Scottish Universities, which is gratefully acknowledged. We are grateful to Britoil, on behalf of the consortium partners, and the UK Department of Energy for giving permission to publish this paper, which is published with the approval of the Director, British Geological Survey (NERC). The line drawing of the seismic section is published by permission of Merlin Geophysical Ltd.

References

- ALLÈGRE C. J., STAUDACHER T. & SARDA P. 1987. Rare gas systematics: formation of the atmosphere, evolution and structure of the Earth's mantle. *Earth and Planetary Science Letters*, **81**, 127–150.
- BROOKS C. K. 1976. The $\text{Fe}_2\text{O}_3/\text{FeO}$ ratio of basalt analyses: an appeal for a standardized procedure. *Bulletin of the Geological Society of Denmark*, **25**, 117–120.
- BURKE W. H., DENISON R. E., HEATHERINGTON E. A., KOEPNICK R. B., NELSON H. F. & OTTO J. B. 1982. Variation of seawater $^{87}\text{Sr}/^{86}\text{Sr}$ throughout Phanerozoic time. *Geology*, **10**, 516–519.
- CUNNINGHAM R. & GILBERT D. 1984. Organic facies of Cenozoic and Cretaceous sediments from Deep Sea Drilling Project sites 549 and 551, northern North Atlantic. In: de GRACIANSKY, P. C. & POAG, C. W. *et al.* *Initial Reports of the Deep Sea Drilling Project*. US Government Printing Office, Washington, **80**, 1073–1079.
- DAMON P. E. & KULP J. L. 1958. Excess helium and argon in beryl and other minerals. *American Mineralogist*, **43**, 443–459.
- DIETRICH V. J. & JONES E. J. W. 1980. Volcanic rocks from Rosemary Bank (Rockall Trough, NE Atlantic). *Marine Geology*, **35**, 287–297.
- ELDHOLM O., THIEDE J., TAYLOR E. *et al.* 1987. *Proceedings of the Ocean Drilling Program*. US Government Printing Office, Washington, **A104**, 783 pp.
- GARIEPY C., LUDDEN J. & BROOKS C. 1983. Isotopic and trace element constraints on the genesis of the Faeroe lava pile. *Earth and Planetary Science Letters*, **63**, 257–272.
- GRACIANSKY P. C. de, AUFFRET G. A., DUPEUBLE P., MONTADERT L. & MULLER C. 1979. Interpretation of depositional environments of the Aptian/Albian black shales of the north margin of the Bay of Biscay (DSDP sites 400 and 402). In: MONTADERT, L., ROBERTS, D. G. *et al.* *Initial Reports of the Deep Sea Drilling Project*. US Government Printing Office, Washington, **48**, 877–907.
- LYLE P. 1985. The petrogenesis of the Tertiary basaltic and intermediate lavas of northeast Ireland. *Scottish Journal of Geology*, **21**, 71–84.
- MACINTYRE R. M. & HAMILTON P. J. 1984. Isotope geochemistry of lavas from sites 553 and 555. In: ROBERTS, P. G., SCHNITKER, D. *et al.* *Initial Reports of the Deep Sea Drilling Project*. US Government Printing Office, Washington, **81**, 775–781.
- MORRISON M. A. 1978. The use of 'immobile' trace elements to distinguish the palaeotectonic affinities of metabasalts: applications to the Palaeocene

- basalts of Mull and Skye, northwest Scotland. *Earth and Planetary Science Letters*, **39**, 407–416.
- , THOMPSON R. N., GIBSON I. L. & MARRINER G. F. 1980. Lateral chemical heterogeneity in Palaeocene upper mantle beneath the Scottish Hebrides. *Philosophical Transactions of the Royal Society of London*, **A297**, 229–244.
- NAYLOR D. & SHANNON P. M. 1982. *The Geology of Offshore Ireland and West Britain*. Graham & Trotman, London, 161 pp.
- NISBET E. G. & PEARCE J. A. 1976. Clinopyroxene composition in mafic lavas from different tectonic settings. *Contributions to Mineralogy and Petrology*, **63**, 149–160.
- PEARCE J. A. 1982. Trace element characteristics of lavas from destructive plate boundaries. In: THORPE R. S. (ed) *Andesites*. Wiley, New York, pp. 525–548.
- & CANN J. R. 1973. Tectonic setting of basic volcanic rocks determined using trace element analyses. *Earth and Planetary Science Letters*, **19**, 290–300.
- PRESTVIK T. 1982. Basic volcanic rocks and tectonic setting: discussion of the Zr-Ti-Y diagram and its suitability for classification purposes. *Lithos*, **15**, 241–247.
- ROBERTS D. G. 1975. Marine geology of the Rockall Plateau and Trough. *Philosophical Transactions of the Royal Society of London*, **A278**, 447–509.
- , MASSON D. G. & MILES P. R. 1981. Age and structure of the southern Rockall Trough. *Earth and Planetary Science Letters*, **52**, 115–128.
- , BOTT M. H. P. & URUSKI C. 1983. Structure and origin of the Wyville–Thomson Ridge. In: BOTT M. H. P., SAXOV S., TALWANI M. & THIEDE J. (eds) *Structure and Development of the Greenland–Scotland Ridge*. Plenum Press, New York, pp. 133–158.
- RUSSELL M. J. & SMYTHE D. K. 1977. Evidence for an early Permian oceanic rift in the northern North Atlantic. In: NEUMANN E. R. & RAMBERG I. B. (eds) *Petrology and Geochemistry of Continental Rifts*. Reidel, Dordrecht, pp. 173–179.
- SAUNDERS A. D. 1984. The rare earth element characteristics of igneous rocks from the ocean basins. In: HENDERSON P. (ed) *Rare Earth Element Geochemistry*, Developments in Geochemistry, **2**, 205–236.
- SHERVAIS J. W. 1982. Ti/V plots and the petrogenesis of modern and ophiolitic lavas. *Earth and Planetary Science Letters*, **52**, 115–128.
- TARNEY J., SAUNDERS A. D., WEAVER S. D., DONNELLAN N. C. B. & HENDRY G. L. 1979. Minor element geochemistry of basalts from Leg 49, North Atlantic Ocean. In: LUYENDYK, B. P., CANN, J. R. et al. *Initial Reports of the Deep Sea Drilling Project*. US Government Printing Office, Washington, **49**, 657–691.
- THOMPSON R. N., GIBSON I. L., MARRINER G. F., MATTEY D. P. & MORRISON M. A. 1980. Trace element evidence of multistage mantle fusion and polybaric fractional crystallization in the Palaeocene lavas of Skye, NW Scotland. *Journal of Petrology*, **21**, 265–293.
- TIMOFEEV P. P. & BOGOLYUBOVA L. I. 1979. Black shales of the Bay of Biscay and conditions of their formation. In: *Initial Reports of the Deep Sea Drilling Project*. US Government Printing Office, Washington, **48**, 831–853.
- VINE F. J. & TOUTELOU E. B. 1970. Geochemistry of black shale deposits—a summary. *Economic Geology*, **65**, 253–273.
- WAAGSTEIN R., HALD N., JØRGENSEN O., NIELSEN P. H., NOE-NYGAARD A., RASMUSSEN J. & SCHOENHARTING G. 1984. Deep drilling on the Faeroe Islands. *Bulletin of the Geological Society of Denmark*, **32**, 133–138.
- WOOD D. A., JORON J-L. & TREUIL M. 1979. A reappraisal of the use of trace elements to classify and discriminate between magma series erupted in different tectonic settings. *Earth and Planetary Science Letters*, **45**, 326–336.
- YORK D. & FARQUHAR R. M. 1972. *The Earth's Age and Geochronology*. Pergamon Press, New York, 178 pp.
- , MACINTYRE R. M. & GITTINS J. 1969. Excess radiogenic ⁴⁰Ar in cancrinite and sodalite. *Earth and Planetary Science Letters*, **7**, 25–28.
- ZARTMAN R. E. & DOE B. R. 1981. Plumbotectonics—the model. *Tectonophysics*, **75**, 135–162.

A. C. MORTON, British Geological Survey, Keyworth, Notts NG12 5GG, UK.

J. E. DIXON, J. G. FITTON, Grant Institute of Geology, University of Edinburgh, West Mains Road, Edinburgh EH9 3JW, UK.

R. M. MACINTYRE, Scottish Universities Research and Reactor Centre, East Kilbride, Glasgow G75 0QU, UK.

D. K. SMYTHE, British Geological Survey, Murchison House, West Mains Road, Edinburgh EH9 5LA, UK.

P. N. TAYLOR, Department of Earth Sciences, University of Oxford, Parks Road, Oxford OX1 3PR, UK.